Supporting Information

Boosting Photoelectrochemical Water Oxidation with Cobalt Phosphide Nanosheets on Porous $BiVO_4$

Haili Tong, Yi Jiang, Qian Zhang, Wenchao Jiang, Kaili Wang, Xiaoxi Luo, Ze Lin, and Lixin Xia**

College of Chemistry, Liaoning University, No. 66, Chongshan Middle Road, Huanggu District,

Shenyang 110036, People's Republic of China

*Corresponding authors.

E-mail addresses: jiangyi@lnu.edu.cn (Y Jiang); lixinxia@lnu.edu.cn (L Xia).

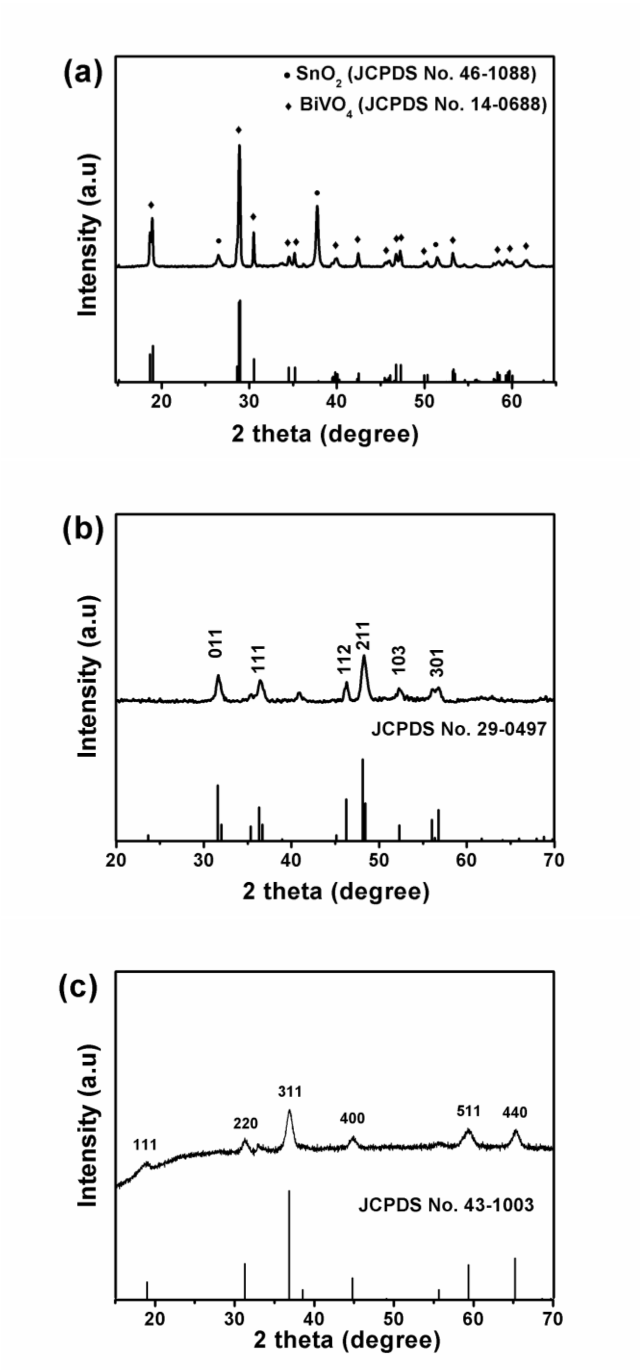

Figure S1. XRD patterns of (a) $BiVO_4$ electrode，(b) CoP powder and (c) Co_3O_4 powder.

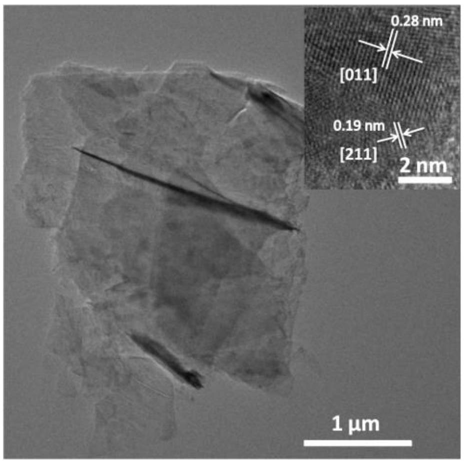

Figure S2. TEM and HRTEM images (inset right) of CoP nanosheets.

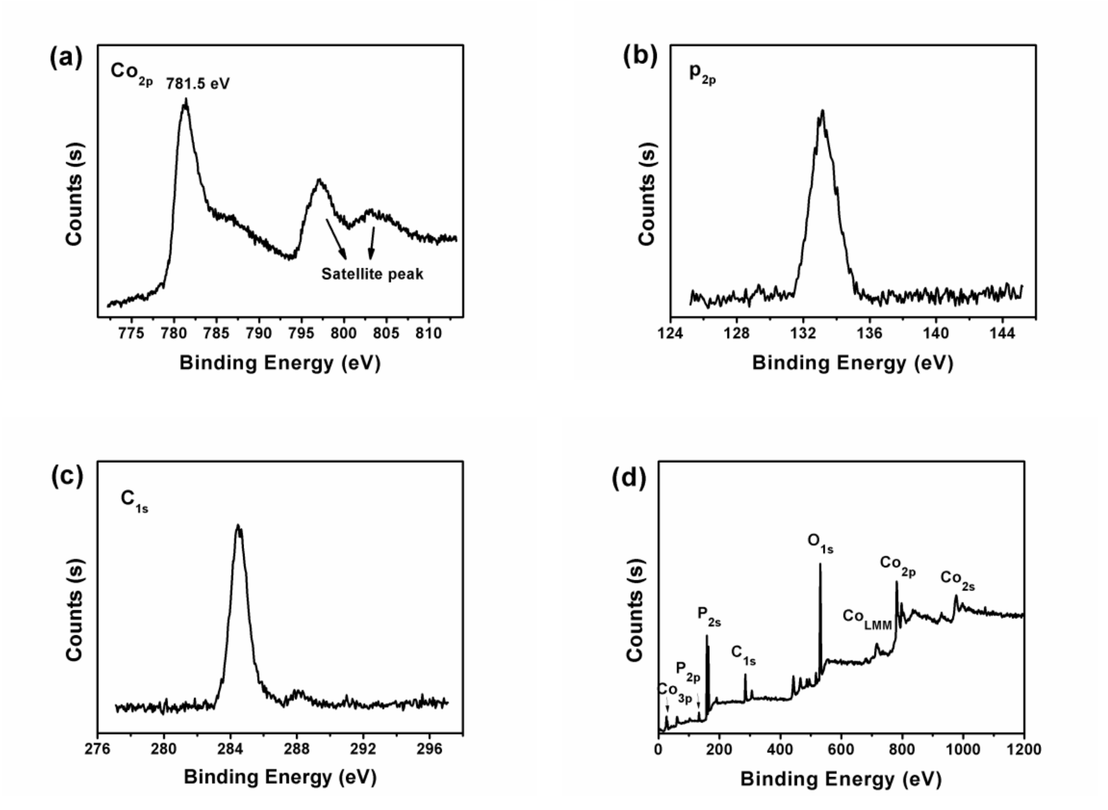

Figure S3. X-ray photoelectron spectroscopy (XPS) spectra of $BiVO_4$+CoP.

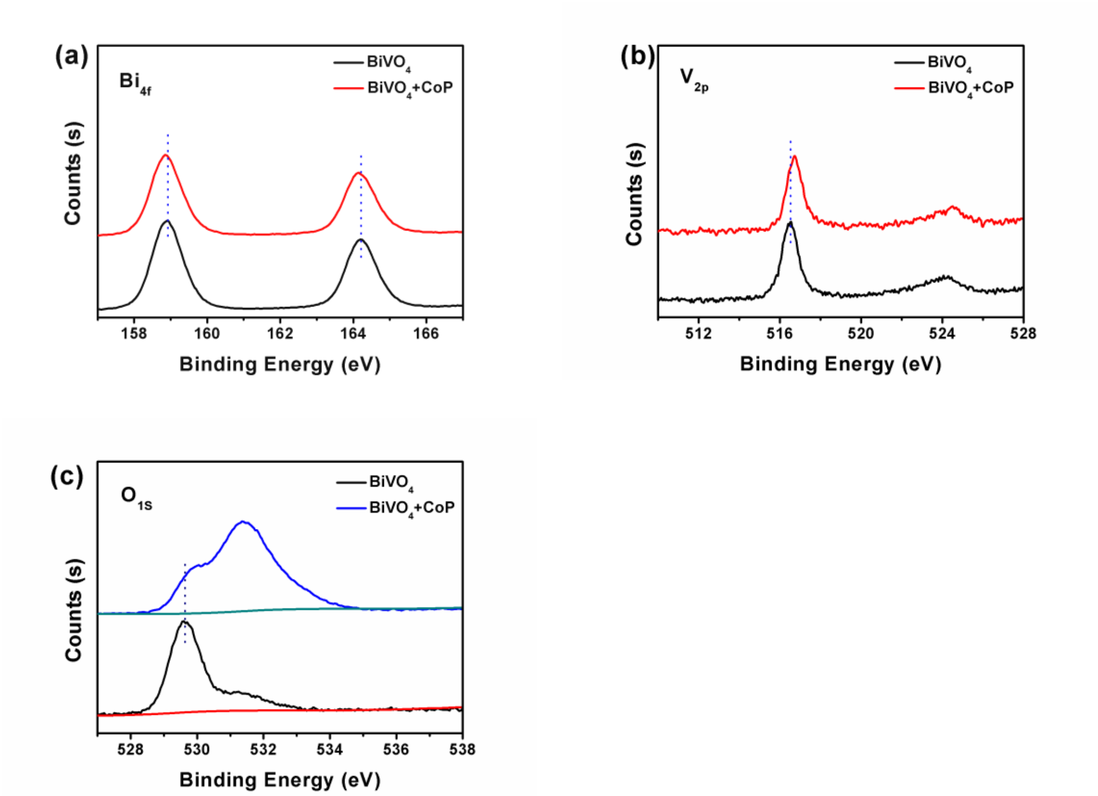

Figure S4. X-ray photoelectron spectroscopy (XPS) detailed spectra over the region of (a) Bi_{4f}, (b) V_{2p} and (c) O_{1s} of $BiVO_4$+CoP.

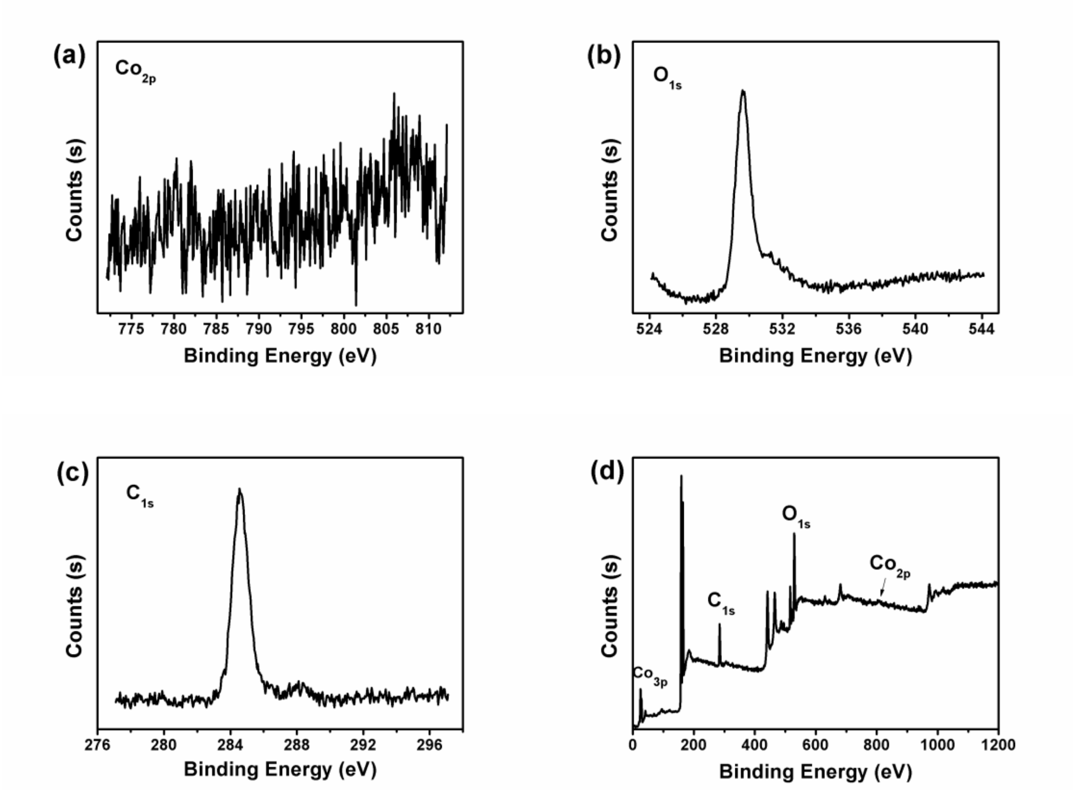

Figure S5. X-ray photoelectron spectroscopy (XPS) spectra of F $BiVO_4$+Co_3O_4.

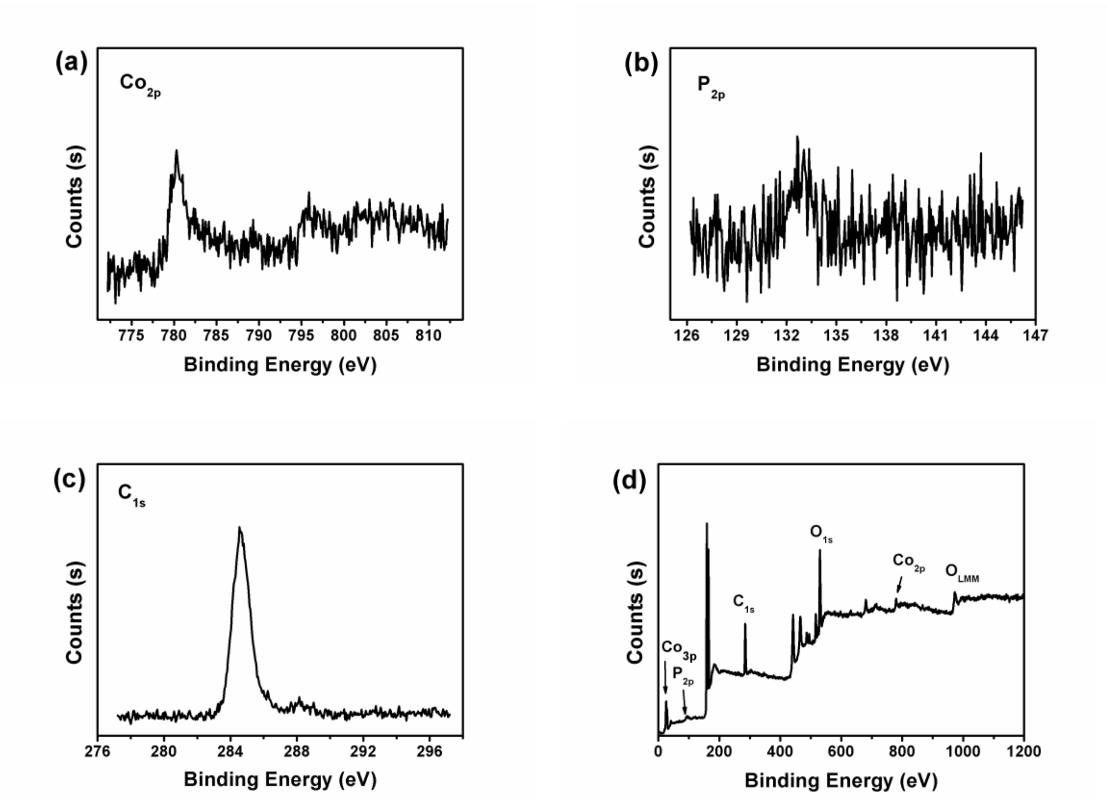

Figure S6. X-ray photoelectron spectroscopy (XPS) spectra of F $BiVO_4$+Co-Pi.

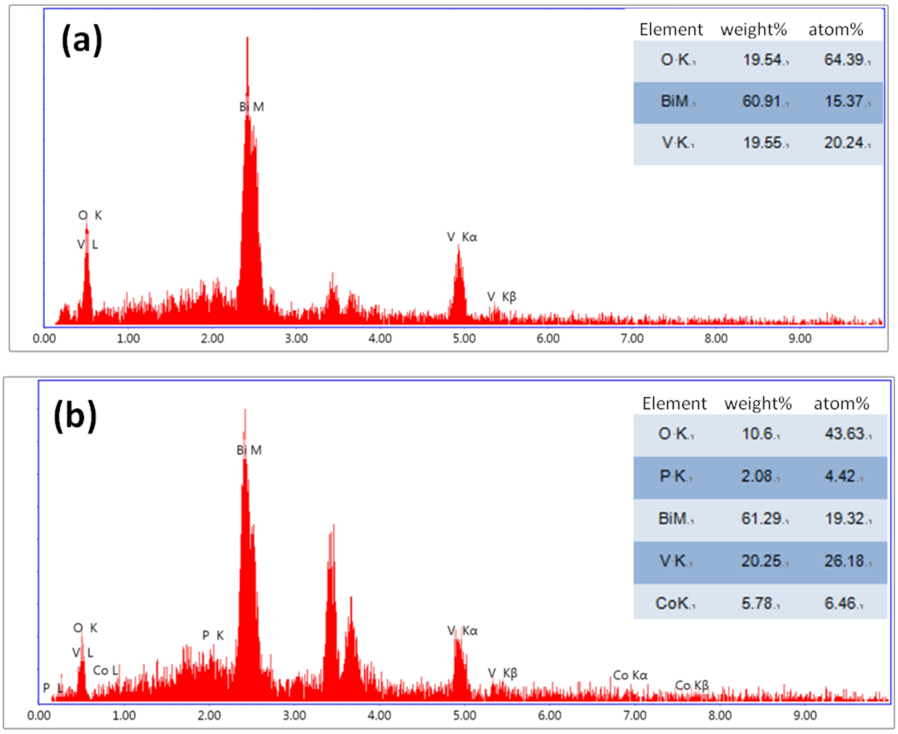

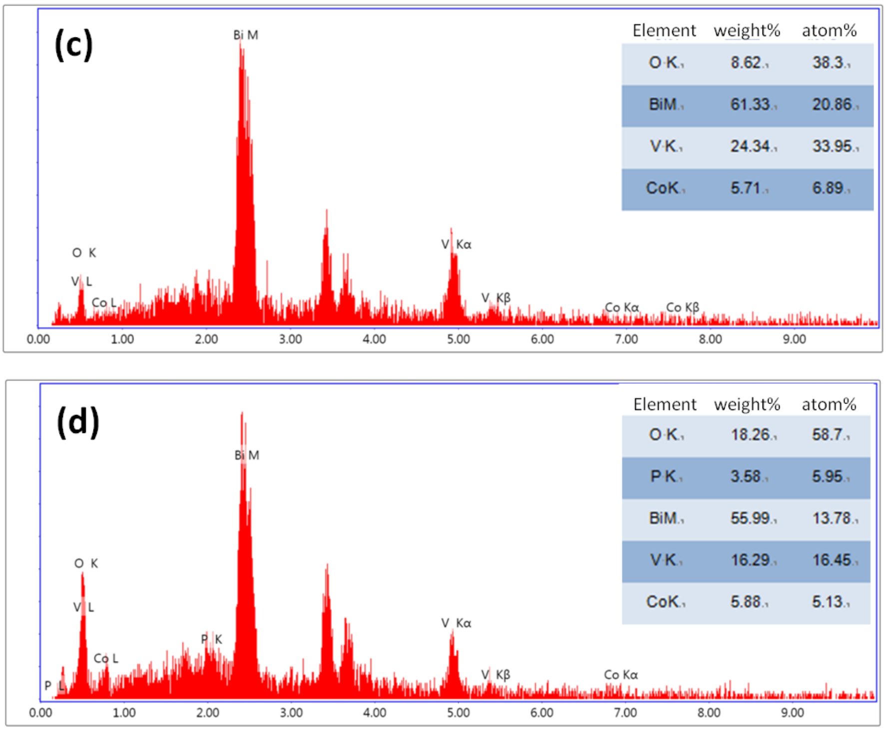

Figure S7. Energy dispersive spectrometry (EDS) of (a) $BiVO_4$, (b) $BiVO_4$+CoP, (c)$BiVO_4$+Co_3O_4 and (d) $BiVO_4$+Co-Pi electrodes.

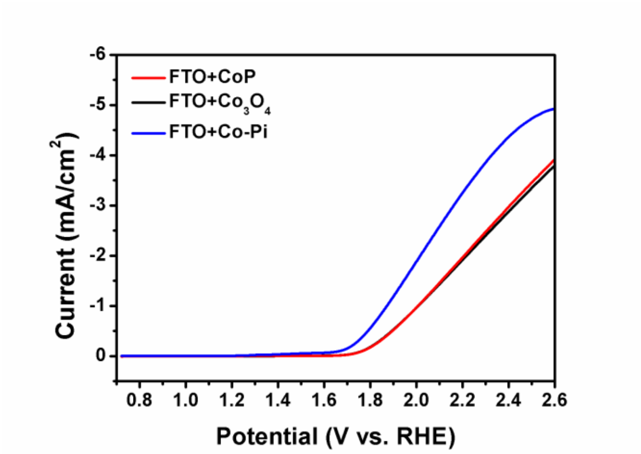

Figure S8. Photocurrent-potential characteristics of FTO+CoP (red); FTO+Co_3O_4 (black) and FTO+Co-Pi (bule) electrodes measured (scan rate, 10 mV/s) under illumination (100 mW/cm^2) in 0.2 M borate buffer (pH 9.0).

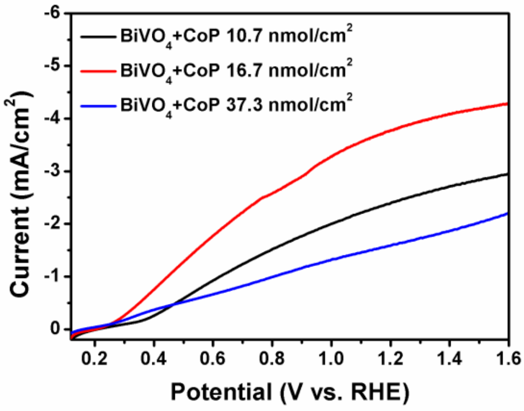

Figure S9. Photocurrent-potential characteristics of $BiVO_4$ photoanode modified by different concentration of CoP in 0.2 M borate buffer (pH 9.0) under illumination (100 mW/cm^2).

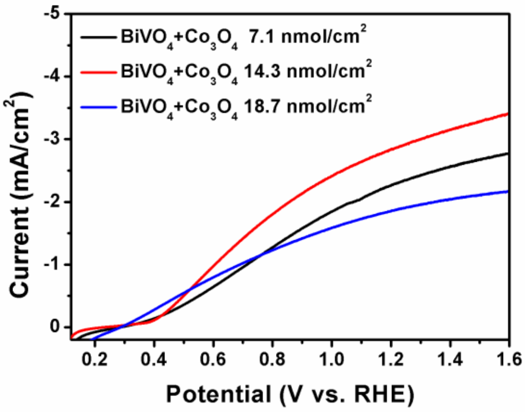

Figure S10. Photocurrent-potential characteristics of $BiVO_4$ photoanode modified by different concentration of Co_3O_4 in 0.2 M borate buffer (pH 9.0) under illumination (100 mW/cm^2).

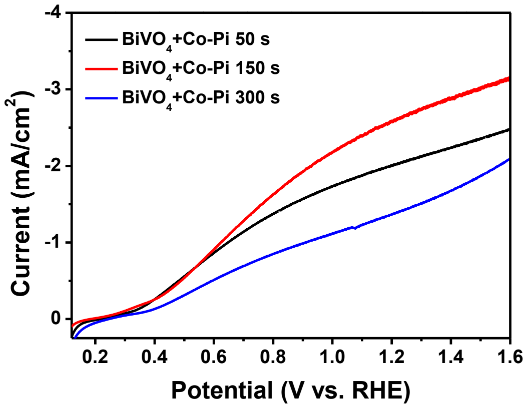

Figure S11. Photocurrent-potential characteristics of $BiVO_4$ photoanode modified by different electrodeposition time of Co-Pi in 0.2 M borate buffer (pH 9.0) under illumination (100 mW/cm^2).

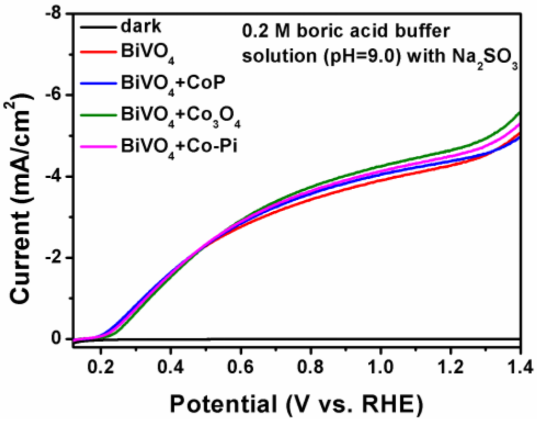

Figure S12. Photocurrent-potential characteristics of $BiVO_4$; $BiVO_4$+CoP; $BiVO_4$+Co_3O_4; $BiVO_4$+Co-Pi electrodes measured (scan rate, 10 mV/s) with and without illumination (100 mW/cm^2) in 0.2 M borate buffer with 1 M Na_2SO_3.

J_{H2O} (the photocurrent of water splitting) is a product of the rate of photon absorption expressed as a $J_{absorbed}$ (current density), $\eta_{charge\ separation}$ is the charge separation efficiency of the photogenerated holes that refer to the bulk recombination, and $\eta_{charge\ injection}$ is charge injection yield of the surface reaching holes into the electrolyte:

$$J_{H_2O} = J_{absorbed} * \eta_{charge\ separation} * \eta_{charge\ injection} \qquad \text{Equation S1}$$

The photocurrent measured in the electrolyte with Na_2SO_3 (J_{Na2SO3}) is only a product of $J_{absorbed}$ and $\eta_{charge\ separation}$, assuming the charge injection yield becomes 100% ($\eta_{charge\ injection}$ = 1) in the presence of a hole scavenger (Na_2SO_3) in the electrolyte:

$$J_{Na_2SO3} = J_{absorbed} * \eta_{charge\ separation} \qquad \text{Equation S2}$$

Based on equation S1 and S2, the charge injection yield can be achieved:

$$\eta_{charge\ injection} = J_{H_2O} / J_{Na_2SO3} \qquad \text{Equation S3}$$

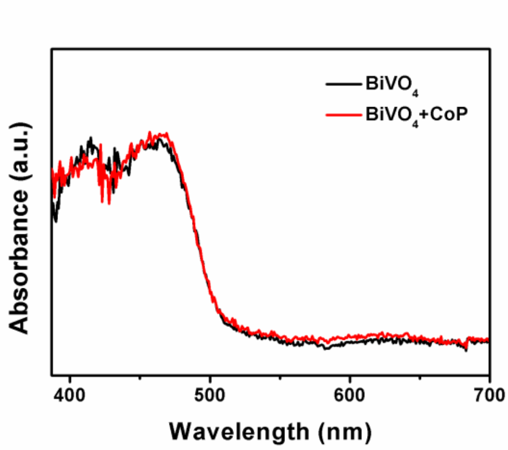

Figure S13. UV-Vis absorption spectra of bare $BiVO_4$ and $BiVO_4$+CoP photoanodes.

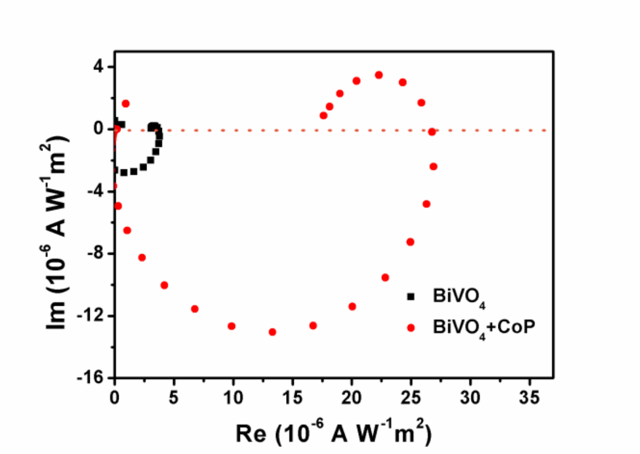

Figure S14. IMPS responses of $BiVO_4$ and $BiVO_4$+CoP photoanodes at 0.9 V vs. RHE.